

Thresholdless nonlinearity-induced edge solitons in trimer arrays

Magnus Johansson^{1, a)}

Department of Physics, Chemistry and Biology (IFM), Linköping University, SE-581 83 Linköping, Sweden

(Dated: 27 February 2025)

We consider a one-dimensional discrete nonlinear Schrödinger (DNLS) model with Kerr-type on-site nonlinearity, where the nearest-neighbor coupling constants take two different values ordered in a three-periodic sequence. The existence of localized edge states in the linear limit (Su-Schrieffer-Heeger trimer, SSH3) is known to depend on the precise location of the edge. Here, we show that for a termination that does not support linear edge states, an arbitrarily weak on-site nonlinearity will induce an edge mode with asymptotic exponential localization, bifurcating from a linear band edge. Close to the gap edge, the shape of the mode can be analytically described in a continuum approximation as one half of a standard gap soliton. The linear stability properties of nonlinear edge modes are also discussed.

I. INTRODUCTION

Recent years have shown a large burst of activity related to topological properties in various physical setups, and in particular within the field of photonics where nonlinear effects often play an important role. For reviews, see, e.g., Refs. 1–4. As a standard one-dimensional model displaying topological features in the linear regime, such as bulk-edge correspondence between existence of edge modes and a nontrivial winding number (Zak phase) of Bloch bands, the Su-Schrieffer-Heeger (SSH) model⁵ is frequently considered. In its simplest version it describes a tight-binding lattice without on-site potential and with binary alternating nearest-neighbor coupling constants, and many works, theoretical as well as experimental, considered the effects of including nonlinear effects of various forms on the topological properties of the SSH model. See, e.g., Ref. 6 and references therein for recent results on the SSH model with cubic (Kerr) or saturable nonlinearities.

An extension of the SSH model that has received increasing attention during the last few years is the SSH trimer (SSH3) model, with a three-site unit cell connected by three alternating coupling constants. In the linear case, several recent works^{7–9} have described properties of edge states and proposed various formulations of a bulk-edge correspondence which, for the most general trimer configurations, is less evident than for the SSH dimer due to absence of mirror-symmetry. Very recently, an acoustic analog of the SSH3 lattices was also proposed, and conditions for existence of edge modes obtained and confirmed experimentally¹⁰. As is known from the above works, the existence of edge states in the SSH3 model depends crucially on the relation between the coupling constants as well as on the location of the edge; a phase diagram for the general case with three different coupling constants was illustrated in Fig. 6 of Ref. 8.

A particular configuration of a trimer array was also studied in the nonlinear regime by Kartashov et al.¹¹

and, using an experimental realization with fs-laser written waveguide arrays, edge solitons were confirmed to bifurcate from linear edge modes in both of the topological gaps of the linear trimer model. Importantly, the implementations studied in Ref. 11 all started with two equal coupling constants closest to the edges, where two linear edge modes exist at each edge only if these two coupling constants are weaker (i.e., with a weakly coupled trimer located at the edge). Qualitatively, the continuations of the linear gap edge modes into nonlinear edge modes were seen to exhibit regimes of instabilities and bifurcations similar to those of the dimer SSH model^{6,12}.

However, if one considers the same bulk trimer configuration as in Ref. 11 but instead terminates the chain with the single strong bond (see Fig. 1 below), a more intricate situation arises. From the phase diagram in Ref. 8 this is seen to correspond to a borderline case where no localized linear edge state exists, but will be created by an arbitrarily weak symmetry breaking if the third bond becomes slightly stronger than the second. It is thus interesting to find out what happens for this configuration if the symmetry between the two weak bonds is preserved, but instead an on-site Kerr nonlinearity added. As we will show here, indeed an arbitrarily weak nonlinearity is sufficient to induce a localized nonlinear edge mode, with frequency bifurcating from the edge of a linear band. Close to the linear band, the edge mode can be described in a continuum approximation using an approach analogous to that used already 30 years ago by Usatenko, Kovalev and Vyalov¹³, who then considered bulk gap solitons in three-atomic elastic chains with anharmonic nearest-neighbor interactions. The small-amplitude edge mode in the nonlinear SSH3 system will take the shape of a standard gap soliton, cut by the edge at its center. This is fundamentally different from the standard SSH model, where nonlinear edge modes bifurcate from the localized linear edge mode at the gap center, and in the continuous limit only consists of a portion of the tail of the corresponding bulk gap soliton^{12,14}.

^{a)} magjo23@liu.se

II. THE NONLINEAR TRIMER MODEL AND ITS LINEAR DISPERSION RELATION

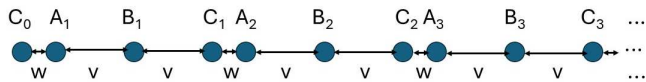


FIG. 1. The configuration of the semi-infinite trimer array.

The semi-infinite trimer array illustrated in Fig. 1 has a three-site unit cell. Labelling site indices with $j = 1, 2, \dots$ and cell indices with $n = 0, 1, 2, \dots$, the following notation for the site amplitudes ψ_j is used (the reason for this choice will become clear later),

$$\begin{aligned}\psi_{3n} &= B_n, \\ \psi_{3n+1} &= C_n, \\ \psi_{3n+2} &= A_{n+1},\end{aligned}\quad (1)$$

with the left edge defined by the boundary condition $B_0 = 0$.

The equations of motion for the SSH3 model with on-site (focusing) Kerr nonlinearity and positive coupling constants v, w can then be written in the standard form

$$\begin{aligned}i\dot{A}_n + wC_{n-1} + vB_n + |A_n|^2 A_n &= 0; n \geq 1, \\ i\dot{B}_n + v(A_n + C_n) + |B_n|^2 B_n &= 0; n \geq 1, \\ i\dot{C}_n + vB_n + wA_{n+1} + |C_n|^2 C_n &= 0; n \geq 0.\end{aligned}\quad (2)$$

The linear spectral bands are obtained in the standard way by neglecting the nonlinear terms and replacing the edge with periodic boundary conditions, $B_0 = B_N, C_N = C_0$. From the ansatz

$$(A_n, B_n, C_n) = (A, B, C)e^{i(kn + \lambda t)},$$

the linear dispersion relation $\lambda(k)$ is determined by the solutions to the cubic equation

$$\lambda^3 - (w^2 + 2v^2)\lambda - 2v^2w \cos(k) = 0, \quad (3)$$

illustrated in Fig. 2. Note that $\lambda(k) = -\lambda(\pi - k)$, with the nonzero eigenvalues at the band center given by $\lambda_{\pm}(k = \pi/2) = \pm\sqrt{w^2 + 2v^2}$. The eigenvalues at the band edges also have simple expressions, $\lambda_-(k = 0) = -w$, $\lambda_0(k = 0) = (w - \sqrt{w^2 + 8v^2})/2$, $\lambda_+(k = 0) = (w + \sqrt{w^2 + 8v^2})/2$. (We here assumed $w > v$, if $w < v$ the eigenvalues λ_- and λ_0 will switch order.)

The linear eigenmode corresponding to the upper edge of the lower band ($k = 0$), with $\lambda = -w$, has the simple structure $A = -C, B = 0$. Thus, this eigenmode is also an exact eigenmode for the semi-infinite chain, and, as we will see below, will yield a localized edge mode with frequency entering the gap in presence of focusing nonlinearity. (Due to the symmetry of the spectrum the same scenario, apart from sign changes, will occur at the lower edge of the upper band if the nonlinearity is defocusing.)

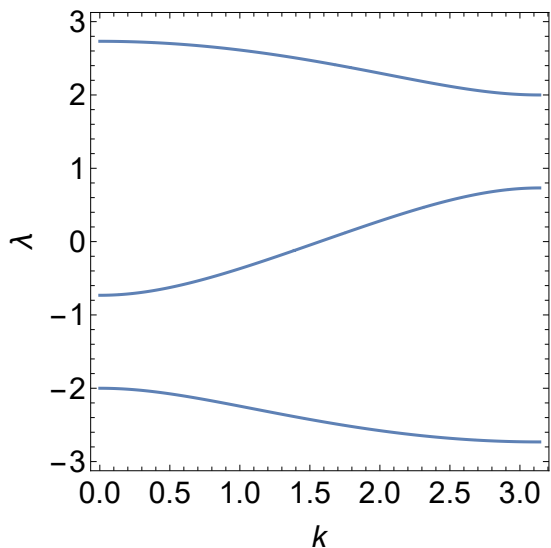


FIG. 2. Dispersion relation (3) with $w = 2, v = 1$.

III. THE NONLINEARITY-INDUCED EDGE MODE

A. Limit of uncoupled dimers

The standard way to construct families of gap modes in various types of nonlinear lattice models consists essentially of three steps: (i) find an “anticontinuous” limit where the system is decoupled and can be solved exactly, and determine an appropriate configuration of its time-periodic solutions with frequency inside the gap of the linear spectrum; (ii) continue the anticontinuous solution for increasing coupling between the units; and (iii) continue the solution for fixed nonzero coupling versus frequency in both directions, to determine whether it reaches the gap edges or bifurcates with some other gap mode inside the gap. In this way, complete families of fundamental bulk gap modes connecting the anticontinuous solutions smoothly to the continuous gap solitons at one band edge, and to nonlocalized “outgap” solitons at the other edge, have been identified e.g. for the DNLS model with binary modulated on-site potentials¹⁵, and for the nonlinear SSH model¹⁶.

Here, the structure of the linear mode at the upper edge of the lower band suggests an appropriate anticontinuous limit $v = 0$, which turns the system into a chain of uncoupled dimers with internal coupling w . This is identical to the uncoupled limit for bulk gap solitons in the standard SSH model¹⁶, and the relevant solution for an edge mode in this limit can be chosen as $C_0 = -A_1 = \sqrt{w + \lambda}e^{i\lambda t}$ with stationary frequency $-w < \lambda < 0$, and all other sites at zero amplitude. An example of a family of nonlinear edge modes resulting from continuing this solution for increasing v is shown in Fig. 3. Analogously to the scenario for the standard nonlinear SSH model¹⁶, the mode remains localized close to the edge until the coupling v reaches a value

where the frequency enters the band above the gap (at $v/w = \sqrt{3/8} = 0.612\dots$ in Fig. 3), where it develops a non-decaying oscillatory tail.

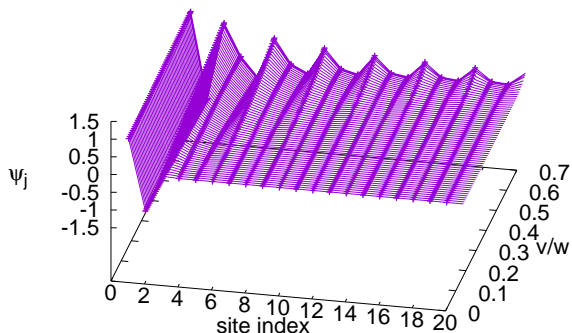


FIG. 3. Continuation of the nonlinear edge mode versus v from the limit $v = 0$ of uncoupled dimers, with fixed $w = 2$ and $\lambda = -1$. Only the part closest to the edge is shown.

Performing the continuation versus frequency at fixed v (here $v/w = 0.5$) it traces out the full continuous family of localized edge modes in the lower gap region, with the transition to a non-localized “out-gap” mode with non-decaying tail at the upper gap edge, and the approach to a small-amplitude continuum-like mode at the lower gap edge. As illustrated in the upper Fig. 4, the norm $P = \sum_j |\psi_j|^2$ describes a monotonously increasing function $P(\lambda)$, approaching zero at the lower gap edge ($\lambda = -2$) and diverging at the upper ($\lambda = -\sqrt{3} + 1 \approx -0.732$.) Thus, the localized nonlinear edge mode appears as a bifurcation from the linear extended mode at the upper edge of the lower band, without excitation threshold. The shape of the mode close to the lower gap edge is illustrated in the lower Fig. 4, and is clearly seen to have a continuous envelope modulation of the linear band edge mode, with the main-field amplitudes (A and C sites) approaching a maximum with zero derivative and the small-field amplitude (B sites) approaching zero at the edge of the chain. Thus, the edge mode has the structure of a “half” bulk gap soliton, cut in the middle by the edge boundary condition. This will be confirmed below by deriving appropriate modulation equations in a continuous approximation.

B. Continuous gap soliton limit

In a continuous approximation of (2) we replace the site index n with a continuous variable $x = n$, and look for stationary solutions of the form

$$(A(x), B(x), C(x))e^{i\lambda t},$$

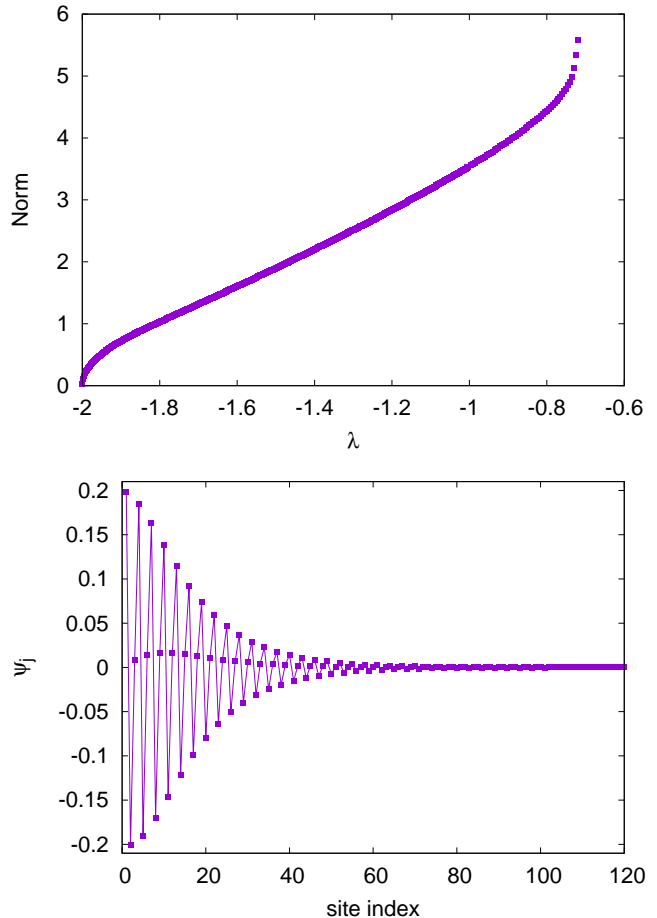


FIG. 4. Upper: Norm versus frequency at fixed $w = 2$, $v = 1$. Lower: Mode amplitudes close to the band edge, $\lambda = -1.98$.

where $A(x), B(x), C(x)$ are slowly varying real-valued functions. Then, to lowest order approximation we replace $A_{n+1} \rightarrow A(x) + dA(x)/dx$, $C_{n-1} \rightarrow C(x) - dC(x)/dx$, turning Eqs. (2) into

$$-\lambda A + wC - w \frac{dC}{dx} + vB + A^3 = 0, \quad (4)$$

$$-\lambda B + v(A + C) + B^3 = 0, \quad (5)$$

$$-\lambda C + vB + wA + w \frac{dA}{dx} + C^3 = 0, \quad (6)$$

with boundary condition $B(0) = 0$. Analogously to the three-atomic elastic chain analyzed in Ref. 13, there are two first-order differential equations for the fields A and C combined with a local algebraic equation for the field B . (As noted in Ref. 13, this structure also generalizes to N -mers yielding $N - 2$ algebraic equations.) Here, as B defines the small-amplitude field we may to lowest order neglect the cubic term in (5) and obtain $B \simeq \frac{v}{\lambda}(A + C)$. Adding and subtracting Eqs. (4) and (6) and defining new functions $f = (A - C)/2$, $\phi = (A + C)/2$ then leads to the system

$$w \frac{d\phi}{dx} = f [(-w - \lambda) + f^2 + 3\phi^2], \quad (7)$$

$$w \frac{df}{dx} = \phi \left[(-w + \lambda - \frac{2v^2}{\lambda}) - (\phi^2 + 3f^2) \right]. \quad (8)$$

These equations are equivalent to the well known gap soliton equations for a diatomic elastic chain whose exact analytical solutions in terms of hyperbolic functions were analyzed in detail by Chubykalo, Kovalev and Usatenko¹⁷, and later extended by Kovalev et al.¹⁸ to more general systems resulting in different coefficients in front of the nonlinear terms as compared to (7)-(8). Here Eq. (7) describes the spatial shape of the small-amplitude field ϕ and (8) that of the large-amplitude field f . The boundary condition at the edge yields $\phi(0) = 0$, which through (8) also implies the boundary condition $\frac{df}{dx}(0) = 0$ for the main field f . Thus, the edge boundary conditions here correspond exactly to the conditions at the center of a standard bulk gap soliton, which explains the shape of the edge mode as a “half” gap soliton shown in Fig. 4 (compare, e.g., with Fig. 2 in Ref. 17). The maximum amplitude for the main field f of the analytical gap soliton is obtained¹⁷ from the linear term in (7) as $f_{max} = \sqrt{2(\lambda + w)}$, which for the parameter values in Fig. 4 yields $f_{max} = 0.2$, in very good agreement with the numerical results. So from the solutions to (7)-(8) we obtain, assuming the continuous approximation to be valid close to the lower gap edge $\lambda \gtrsim -w$, $A_n \approx \phi(x) + f(x)$, $B_n \approx -\frac{2v}{w}\phi(x)$, $C_n \approx \phi(x) - f(x)$.

We should note that in deriving (7)-(8) we made slightly different assumptions than in Refs. 13, 17, and 18. (i) We did not assume the gap width (here given by $(3w - \sqrt{w^2 + 8v^2})/2$) to be small. This limits the validity of our continuous approximation to the regime close to the lower band edge, $\lambda \gtrsim -w$, and in particular the transition to “outgap” edge soliton at the upper gap edge is generally not accurately described by (7)-(8). (ii) We neglected the cubic term in the small-amplitude field B in (5). A more accurate approximation yields $B = \frac{2v}{\lambda}\phi + \frac{8v^3}{\lambda^4}\phi^3 + \mathcal{O}(\phi^5)$. Including also the last term will shift the coefficient for the ϕ^2 term in (8) from unity to $1 + 8(\frac{v}{\lambda})^4$, which does not change qualitatively the shape of the solution since $\phi^2 \ll 3f^2$ when the soliton amplitude is non-negligible (the effect of changing this coefficient was discussed in Ref. 18). Quantitatively, we do however observe some deviations between the predictions from the continuum model and the numerically calculated exact edge modes, as concerns the amplitude and location of the peak of the small-amplitude field B . This is likely due to the neglect of higher derivatives in (4)-(6).

IV. LINEAR STABILITY

Considering the stability of the family of nonlinear edge modes, we perform a standard numerical linear stability analysis (cf. e.g. Refs. 15,16). Expressing an exact stationary edge mode as $\psi_j(t) = \psi_j^{(\lambda)} e^{i\lambda t}$, with $\psi_j^{(\lambda)}$ time-independent, the linear stability is determined by adding a small perturbation written in the form $\psi_j(t) = [\psi_j^{(\lambda)} + \epsilon_j(t)] e^{i\lambda t}$, with $\epsilon_j(t) = \frac{1}{2}(\xi_j + \eta_j) e^{-i\omega_l t} + \frac{1}{2}(\xi_j^* - \eta_j^*) e^{i\omega_l^* t}$. Linearizing and solving the resulting eigenvalue problem yields the small-amplitude oscillation frequencies ω_l , with linear stability requiring all ω_l to be real.

The linear stability properties for three different values of v/w are illustrated in Fig. 5. Qualitatively, the pictures show strong resemblance with the corresponding stability properties for bulk gap solitons in the standard (dimer) SSH model¹⁶. As seen from the bottom plots in Fig. 5, the edge modes are always linearly stable in the lower part of the gap (small-amplitude regime), while oscillatory instabilities (complex eigenvalues) generally develop in the upper part. By comparing with the top plots for the real parts of oscillation frequencies, we see that the stronger instabilities appear when isolated eigenvalues, bifurcating from some subband and corresponding to localized internal mode oscillations, resonate with band eigenvalues (extended eigenmodes corresponding to a continuous spectrum in the limit of infinite system size) from some other subband. The broad spectrum of very weak instabilities is a standard signature of overlapping continuous spectra, yielding finite-size instabilities with strength decaying towards zero as system size increases. It is also interesting to note that for smaller values of v/w the edge mode regains stability close to the upper gap edge, while the instability persists for larger v/w . Similar features are seen both for bulk gap¹⁶ and edge^{6,12} solitons in the dimer SSH model.

Another interesting feature seen in Fig. 5, analogous to bulk gap solitons in dimer SSH, is the presence of a localized mode with purely real eigenfrequency above all continuous bands. In fact, in the limit $v \rightarrow 0$ this mode is the same symmetric eigenmode ($\epsilon_1 = \epsilon_2$) found in Ref. 16, now localized at the edge sites and having eigenfrequency $\omega_l = 2w\sqrt{\frac{\lambda}{w} + 2} + \mathcal{O}(v^2)$. As the upper edge of the spectrum of extended eigenmodes for small v is located at $\omega_l = w - \lambda + \mathcal{O}(v^2)$, it follows directly that this eigenmode is located above all continuous bands for all λ in the gap when v is small. As the numerical results in Fig. 5 indicate, the mode indeed stays above the bands also for increasing v . Thus, as also all higher harmonics of this eigenmode will reside above the continuous spectrum, we expect that also “edge breathers” with time-periodically oscillating intensity will exist as exact, non-radiating solutions. Such edge breathers were explicitly found for the dimer SSH model in Ref. 19. An essential difference is that edge breathers in the dimer SSH result from eigenmodes in the gap, which make them more prone to instabilities and resonances. The edge breathers in the

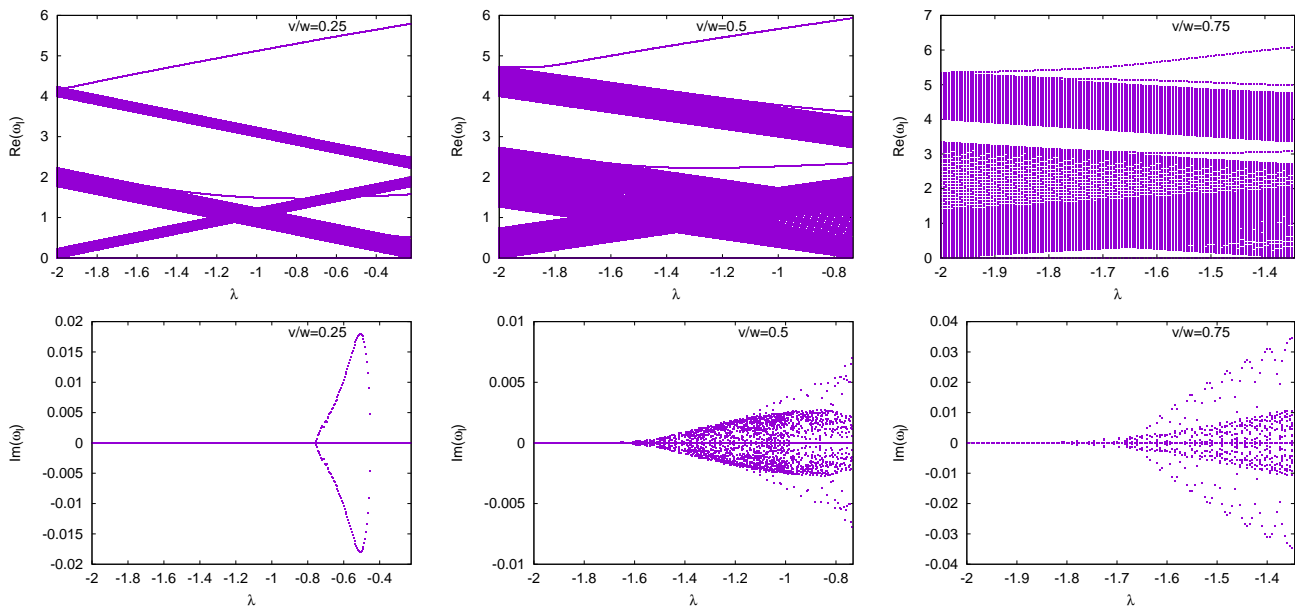


FIG. 5. Real and imaginary parts of the linear stability eigenfrequencies for three values of v/w as indicated in the figures, with $w = 2$ and $N = 40$ unit cells. Only the upper half (positive real part) of the spectrum is shown in the top plots.

trimer SSH model, resulting from an eigenmode above the continuous spectrum, are expected to exist stably in a larger domain, more similar to the “pulsons” resulting from a similar eigenmode for bulk gap solitons in the model with binary modulated on-site potential²⁰.

V. CONCLUSIONS

In conclusion we presented a model system, a trimer array (SSH3) starting with a single strong bond followed by two weak bonds, which does not support localized edge modes in the linear limit but where an arbitrarily weak on-site nonlinearity is sufficient to induce a thresholdless localized nonlinear edge mode, without explicitly breaking the symmetry of the chain. We showed that, close to the gap edge from which it bifurcates, the mode envelope could be approximated by exactly one half of a continuous bulk gap soliton. The linear stability of the edge mode also indicated a similar scenario as for bulk gap solitons in the standard SSH model, with stability for smaller amplitude and regimes of oscillatory instabilities appearing with increasing amplitude. We also pointed out that conditions for existence of time-periodically oscillating, localized edge breathers are generically fulfilled for the full range of parameter values. These phenomena may be experimentally observed e.g. with setups similar to those used in Ref. 11.

ACKNOWLEDGMENTS

It is a pleasure to contribute this work to the celebration of the 80th birthday of Alexander Kovalev, among many other things pioneer in the study of gap solitons in nonlinear lattices. Our joint collaboration projects had a strong impact on the activities of our group, and I have highly appreciated his deep knowledge in nonlinear physics, as well as his personal kindness and generosity.

- ¹D. Smirnova, D. Leykam, Y. Chong, and Y. Kivshar, “Nonlinear topological photonics”, *Appl. Phys. Rev.* **7**, 021306 (2020).
- ²M.J. Ablowitz and J.T. Cole, “Nonlinear optical waveguide lattices: Asymptotic analysis, solitons, and topological insulators”, *Physica D* **440**, 133440 (2022).
- ³S. Kruk, “Nonlinear topological photonics”, in: G. C. Righini, L. Sirlito (Eds.), *Advances in Nonlinear Photonics*, Woodhead Publishing Series in Electronic and Optical Materials, Woodhead Publishing, 2023, pp. 85–111.
- ⁴A. Szameit and M.C. Rechtsman, “Discrete nonlinear topological photonics”. *Nature Physics* **20**, 905 (2024).
- ⁵W.P. Su, J.R. Schrieffer, and A.J. Heeger, “Solitons in Polyacetylene”, *Phys. Rev. Lett.* **42**, 1698 (1979).
- ⁶K. Bugarski, A. Maluckov, R.A. Vicencio and M. Johansson, “Edge modes in strongly nonlinear saturable SSH photonic lattices: Tracing a bulk-edge correspondence through instabilities and bifurcations”, *Chaos, Solitons & Fractals* **193**, 116086 (2025).
- ⁷V.M. Martinez Alvarez and M.D. Coutinho-Filho, “Edge states in trimer lattices”, *Phys. Rev. A* **99**, 013833 (2019).
- ⁸A. Anastasiadis, G. Styliaris, R. Chaunsali, G. Theocharis, and F.K. Diakonov, “Bulk-edge correspondence in the trimer Su-Schrieffer-Heeger model”, *Phys. Rev. B* **106**, 085109 (2022).
- ⁹T. Jiang, J. Zhang, G. Xin, Y. Dang, A. Xiang, X. Qi, W. Zhang, and Z. Yang, “Topological oscillated edge states in trimer lattices”, *Opt. Express* **32**, 18605 (2024).
- ¹⁰I. Ioannou Sougleridis, A. Anastasiadis, O. Richoux, V. Achilleos, G. Theocharis, V. Pagneux, and F. K. Diakonov, “Existence and

- characterization of edge states in an acoustic trimer Su-Schrieffer-Heeger model”, *Phys. Rev. B* **110**, 174311 (2024).
- ¹¹Y.V. Kartashov, A.A. Arkhipova, S.A. Zhuravitskii, N.N. Skryabin, I.V. Dyakonov, A.A. Kalinkin, S.P. Kulik, V.O. Kompanets, S.V. Chekalin, L. Torner, and V.N. Zadkov, “Observation of Edge Solitons in Topological Trimer Arrays”, *Phys. Rev. Lett.* **128**, 093901 (2022).
- ¹²Y.-P. Ma and H. Susanto, “Topological edge solitons and their stability in a nonlinear Su-Schrieffer-Heeger model”, *Phys. Rev. E* **104**, 054206 (2021).
- ¹³O.V. Usatenko, A.S. Kovalev, and A.A. Vyalov, “Gap solitons in di- and three-atomic elastic chains; the first steps on the way to quasiperiodicity”, in: A.R. Bishop, S. Jiménez, L. Vázquez (Eds.), *Fluctuation Phenomena: Disorder and Nonlinearity - Proceedings of the International Workshop* (World Scientific, Singapore, 1995) pp. 286–291.
- ¹⁴D.A. Smirnova, L.A. Smirnov, D. Leykam, and Y.S. Kivshar, “Topological Edge States and Gap Solitons in the Nonlinear Dirac Model”, *Laser Photonics Rev.* **13**, 1900223 (2019).
- ¹⁵A.V. Gorbach and M. Johansson, “Gap and out-gap breathers in a binary modulated discrete nonlinear Schrödinger model”, *Eur. Phys. J. D* **29**, 77 (2004).
- ¹⁶R.A. Vicencio and M. Johansson, “Discrete gap solitons in waveguide arrays with alternating spacings”, *Phys. Rev. A* **79**, 065801 (2009).
- ¹⁷O.A. Chubykalo, A.S. Kovalev and O.V. Usatenko, “Dynamical solitons in a one-dimensional nonlinear diatomic chain”, *Phys. Rev. B* **47**, 3153 (1993).
- ¹⁸A.S. Kovalev, O.V. Usatenko, and A.V. Gorbach, “Bifurcation picture for gap solitons in nonlinear modulated systems”, *Phys. Rev. E* **60**, 2309 (1999).
- ¹⁹M. Johansson, “Topological edge breathers in a nonlinear Su-Schrieffer-Heeger lattice”, *Phys. Lett. A* **458**, 128593 (2023).
- ²⁰M. Johansson and A.V. Gorbach, “Quasiperiodic localized oscillating solutions in the discrete nonlinear Schrödinger equation with alternating on-site potential”, *Phys. Rev. E* **70**, 057604 (2004).